Integration of oxycombustion and microbial electrosynthesis for sustainable energy storage

Ruth Diego-García[a c], Antonio Morán[a], Luis M. Romeo[b]

[a] Chemical and Environmental Bioprocess Engineering Group, Natural Resources Institute (IRENA), Universidad de León, Av. Portugal, 41, 24009 León, Spain

[b] School of Engineering and Architecture, Department of Mechanical Engineering, Universidad de Zaragoza, Campus Río Ebro, María de Luna 3, 50018, Zaragoza, Spain

[c] Fundación Ciudad de la Energía (CIUDEN), Cubillos del Sil (León), Spain

ABSTRACT

Power-to-gas technology makes use of surplus electricity by its conversion and storage in the form of a gas. Currently *power-to-gas* schemes based on biological processes are of great interest. Microbial electrosynthesis (*MES*) cells are biological systems that produce biogas via microbial action and a supply of electrical energy. The *OxyMES* scheme proposed is a *power-to-gas* system that seeks to neutralize the CO_2 emissions of a standard industrial process through the hybridization of oxy-fuel combustion and bioelectrochemical processes that produce CH_4 (in cathode) and O_2 (in anode). This oxygen is used for oxycombustion in an industrial C-fuel boiler. The energy balance analysis yielded a *power-to-gas* efficiency in the *MES* cell close to 51%, and the overall performance of the *OxyMES* integrated system was close to 60% for a cell with a Faradaic efficiency of 80%, CO_2-to-CH_4 conversion rate of 95%, and ΔV_{cell} = 1.63 V. With the proper sizing of the CO_2, O_2, and biogas process tank system, it is possible to achieve 100% autonomy, free from external feedstock supplies.

Keywords: Power-to-Gas; CO_2 conversion; Oxycombustion; Microbial electrosynthesis; Integration; Renewable energy surplus.

Corresponding author's (*): +34 987 291 841

e-mail address: amorp@unileon.es (A. Moran); rdiegg00@estudiantes.unileon.es (R. Diego)

1. INTRODUCTION

According to the IEA, the *net-zero emissions* target for 2050 is to achieve a 45% reduction in total CO_2 emissions by 2030 compared 2010 [1]. The Paris Agreement and recent European commitments also force implementation of an important increase in the contribution of renewable energy sources (RES) for the next years [2]. In the case of EU, this should reach at least 40% of the final gross energy consumption [3].

For the rapid implementation of renewable energies in the electrical system to be viable, they need to be deployed alongside energy storage technologies that enable their integration into the electrical system, minimizing an electricity surplus and ensuring the operability of the system [4]. *Power-to-gas* technology (PtG), which makes use of the renewable electricity surplus of the system by storing it in the form of gas through electrolysis [5], is a sound alternative for energy storage. It allows the interconnection and transfer of energy between the electrical and the gas systems [6]. Also, it provides both with the possibility of increasing their capacity factor and flexibility and improves their ability to adapt to demand, thus expanding profitability options by participating in other electricity market services [7].

In 2016, emissions from energy use in industry accounted for 24.2% of the total of 49.4 $GtCO_{2eq}$ [8]. Certain carbon-based industries will need to adapt their processes to neutralize their emissions. The *power-to-gas* systems allow converting a current fossil fuel-

based gas system into a system that operates with, for instance, biologically derived gases generated with renewable sources, thus getting closer to a more environmentally sustainable energy model and circular economy [9]. In addition, they reduce the energy dependence on external sources, gaining robustness in the sphere of geostrategy events [2]. In this context, locally generated *power-to-gas* schemes based on biological subprocesses have been identified as being of great interest. Among them, one of the most promising options for converting electrical energy surplus is the use of microbial systems [10]. Microbial electrosynthesis (*MES*) cells are biological systems that produce biogas as a result of microbial action and the supply of electrical energy. They are based on the fact that some microorganisms, such as methanogens, have the natural ability to use CO_2 to produce organic compounds [11]. It has been found that genera such as *Geobacter*, *Clostridium,* and *Sporomusa* act as biocatalysts by accepting electrons from a solid electrode to reduce CO_2 directly or indirectly into organic compounds such as methane [12] according to Eq. 1:

$$CO_2 + 8H^+ + 8e^- \Longrightarrow CH_4 + 2H_2O \qquad E0' = -0.24\text{V vs SHE} \qquad \text{[Eq. 1]}$$

The transfer of electrons between microbes and electrodes can be via direct electron transfer (DET) or indirect (IET) transfer or through soluble electron acceptors acting as mediators (MET) [13, 14]. The ability of microorganisms to produce methane by reducing CO_2 using an electrode acting as a direct electron donor was first referenced by Cheng et al. [15]. During the electrochemical interactions of the cathode, hydrogen is produced either by the bioelectrochemical processes of certain microorganisms or by electrolysis reactions when applying a potential in the cathode immersed in an aqueous electrolyte. Also, reducing conditions in a continuous anaerobic reactor may result in an improvement of biotransformation performance compared to a single reducing condition in a substrate-limited batch experiment [16]. Hydrogen can act as an electron donor in CO_2 reduction

reactions, thus promoting indirect electron transfer (IET). Depending on the potential applied to the cathode, one of the electron transfer mechanisms (DET vs. IET) is favoured, although this parameter also influences the methane production obtained [12]. Villano et al. [14] and Gomez et al. [17] observed that a biocathode improves current densities compared to an abiotic cathode that only produces hydrogen.

MES cells mainly consist of two electrodes (anode and cathode) immersed in an aqueous electrolyte and an electroactive biofilm on the cathode (biocathode) with microorganisms that electrocatalyse the CO_2 reduction reaction. A proton-exchange membrane (PEM) is also used to separate the anodic and cathodic chambers. The electrode in the anodic chamber is usually a mesh or sheet of some metallic material such as Ti/IrO_2. Fig. 1 shows a basic diagram of an *MES* cell.

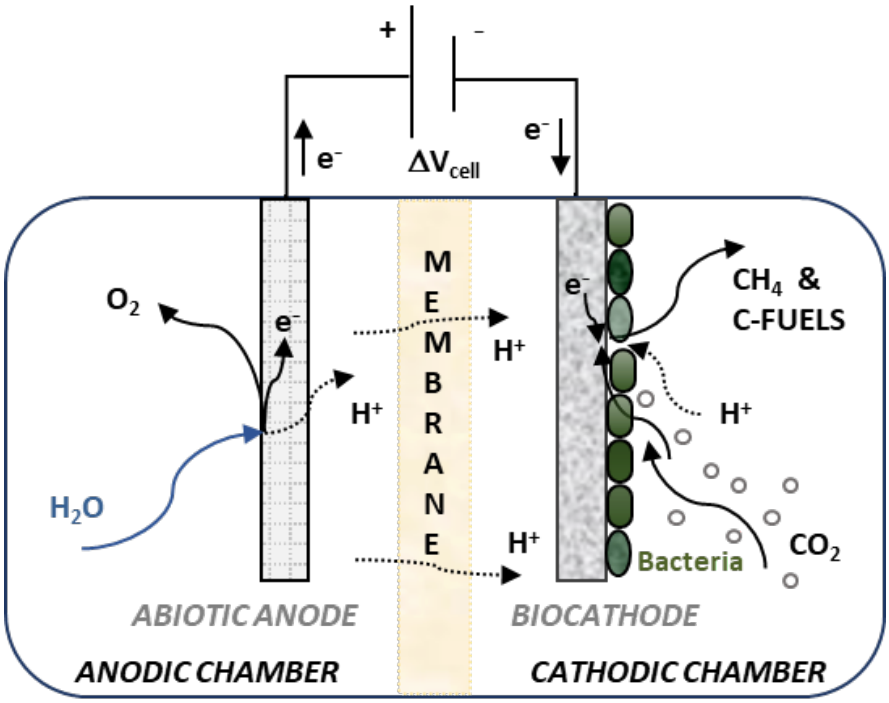

***Fig. 1**. Schematic representation of MES. Adapted from Bajracharya, et al [12]*

The *MES* system can be integrated as a fundamental part of a *power-to-gas* system with energy storage and utilization. It aims to neutralize the emissions of an industrial process

93 throughout the hybridization of oxy-fuel combustion and bioelectrochemical processes.
94 The use of CO_2 emissions in biological systems that convert them into products with
95 energetic value (biogas) is being pursued. In this way, the application of different
96 thermodynamic cycles with various heat recovery strategies for electricity generation are
97 current proposals [18]. Certain designs of *MES* cells, such as the one proposed, allow
98 obtaining pure oxygen as a by-product in the anodic chamber, which is precisely what is
99 used in the boiler during oxycombustion [19]. The innovation of the present work relies on
100 this integration.
101 The integrated operation of both an oxyfuel plant and a *MES* cell have not been analysed
102 jointly so far. There are references of hybridization schemes of oxyboilers [20, 21], clinker
103 kilns [22], and MSW incinerators in *power-to-gas* systems [23]. All of these are based on
104 industrial systems which are of non-biological origin. In the *P2G-BioCat* project [24],
105 hydrogen from an electrolyzer and CO_2 are methanized by microorganisms in a biological
106 reactor; the biomethane produced is injected into the gas grid [25]. In all of these cases, an
107 electrolyser and a methanation reactor are needed to convert electricity to synthetic fuels.
108 State-of-art electrolyser efficiency is around 70% [5], and part of the energy in a
109 methanation reactor is released as heat. This makes the overall efficiency of electricity-to-
110 fuel to be around 55%. To close the research gap, we propose to design a process that
111 avoids the necessity of electrolysers and catalyst reactors to produce synthetic fuels. In this
112 work the process is based on biological systems with microbial electrosynthesis cells.
113 The main objective of the process proposed based on *MES* is to take advantage of the
114 surplus of non-dispatchable renewable energy for its use as an energy source for a
115 microbial electrosynthesis system that recovers industrial CO_2 and produces storable
116 biogas that is suitable for use. That is, there is a twofold final objective: energy storage
117 with zero CO_2 emissions or, in other words, *environmentally sustainable energy storage*.

This work presents the novel concept, the basic sizing of the main equipment necessary, and the overall process efficiency. Although the technological development of the *MES* cell is less advanced than the rest of the hybridized processes, the study shows the potential of this technology when its development accelerates. The integration of conventional energy production systems (boilers) with novel bio-based systems (microbial electrosynthesis cells) presumes the main challenges to be addressed in this type of hybrid scheme.

2. DESCRIPTION OF THE PROPOSED PROCESS: OXYMES

The main units integrating the proposed process are explained in this section. Each unit's description defines the main fluid processes (inlets/outlets), their conditions, and the key functionality parameters. After this, several scenarios are proposed for analysing the individual and global efficiency as a function of three main *MES* operational indicators: electrode potential, faradaic efficiency, and CO_2 conversion rate. The energy analysis will be based on the assumptions made under these *MES* parameters.

As a basic condition for the *OxyMES* design, it has been chosen that global emissions are zero and that the system is as self-sufficient as possible, regarding main feedstock supplies. These two hypotheses influence the design and sizing of the different main units that make up the *OxyMES* scheme. The condition of a self-sustaining system necessarily implies the use of storage tanks for the process fluids (oxygen and biogas) and eliminates their external supplies, especially oxygen.

The process integrates an oxycombustion plant (oxyboiler) with a microbial electrosynthesis system (*MES*). The diagram of the proposed process is schematically illustrated in Figure 2. The process combines the use of surplus renewable electricity with the capture of CO_2 emissions generated in industrial processes through the integration of

143 biomethanization and oxy-fuel combustion processes. With this, it is possible to store the
144 electricity surplus in the form of a biogas for its subsequent storage and delivery to the
145 natural gas network or for any other use.
146 The oxy-fuel boiler provides gases with a high concentration of CO_2 to the *MES* cell while
147 generating steam for heating purposes and/or electricity production. In the cathodic
148 chamber of the *MES* cell, CO_2 from the oxy-flue gases (OxyFG) is converted into methane.
149 This methane forms, together with the rest of the minor OxyFG compounds, a *biogas*.
150 Likewise, the anodic chamber produces a stream of pure oxygen that is used in the boiler
151 for oxy-fuel combustion, avoiding the air separation unit (ASU) that is present in the
152 typical designs for this type of industry [26].
153 The CO_2 gases from the industrial oxy-fuel combustion process are thus recovered as
154 methane, forming a biogas fuel that can be totally or partially injected into the gas network
155 once its composition has been adjusted to the quality requirements of the gas system [27].
156 The design of the *OxyMES* system includes oxygen and biogas storage tanks.

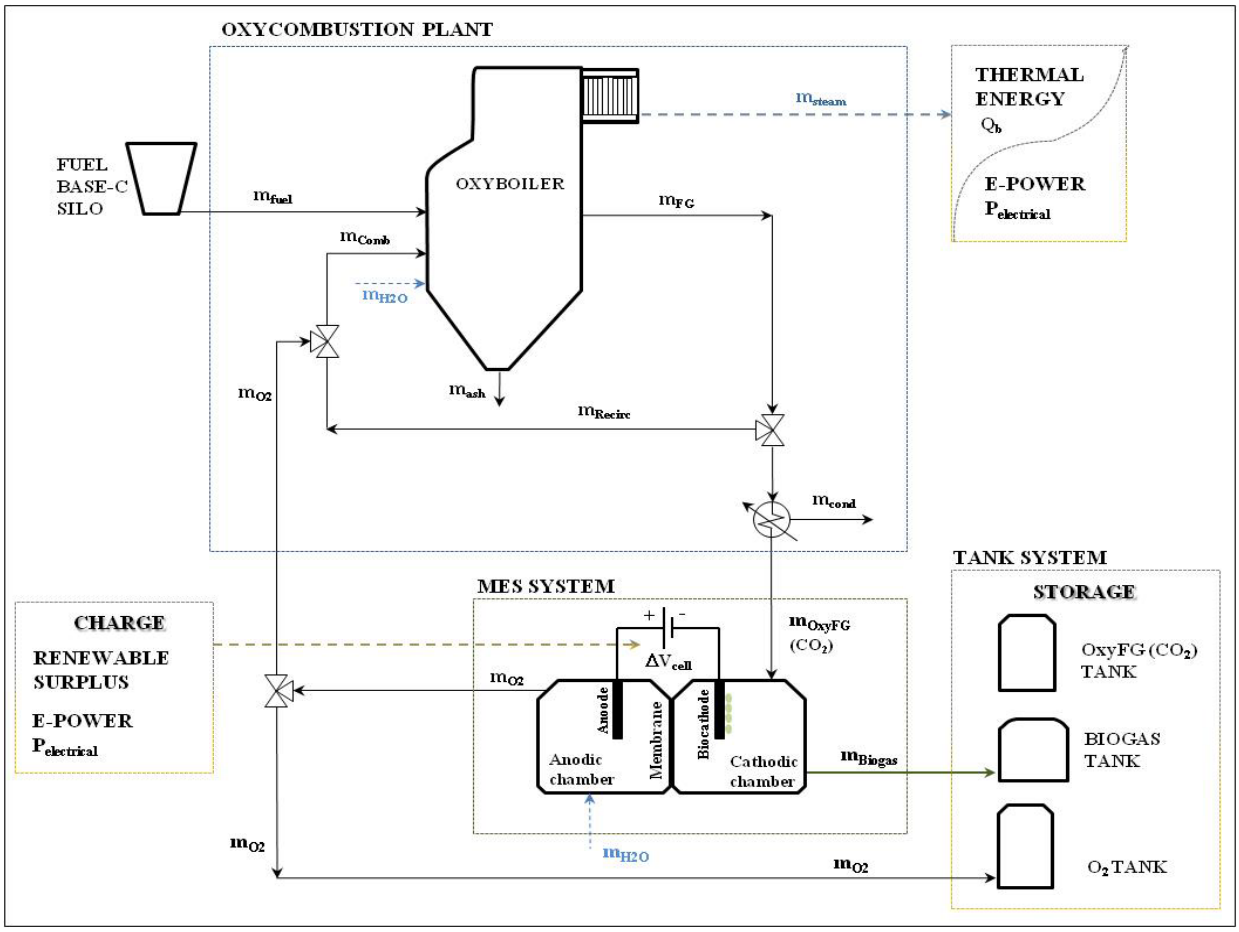

157

158 ***Fig. 1****. Basic scheme for the novel process proposed, 'OxyMES', integrated by three main sub-units:*

159 *Oxyboiler, MES cell, and tanks system (boundary limits marked in dashed lines).*

160

161 **2.1. Oxyfuel boiler**

162 This study is based on the design of a semi-industrial demonstration plant, which has a

163 pulverized coal boiler with a nominal power input of 20 MW_{th}, as well as the rest of the

164 auxiliary systems necessary for its operation (preparation fuel unit, oxidizers, etc.). This

165 plant is located in the Technology Development Center of the *Fundación Ciudad de la*

166 *Energía* (CIUDEN) located in Cubillos del Sil (León, Spain) [28]. The operating data of

167 the oxycombustion plant were obtained during the tests carried out in the framework of the

168 FP7 European co-funded project, *RELCOM* Project [29]. The experimental tests used

169 bituminous coal of South African origin, whose characteristics are reflected in Table 1 of

170 the supplementary material. This flue gas composition was used for the *OxyMES* process

171 simulation. The plant performed tests both in conventional combustion, with air as
172 oxidizer, and in the oxycombustion mode, with different degrees of flue gases recirculating
173 towards the boiler and mixed with pure oxygen (> 99.5% purity) supplied from cryogenic
174 liquefied oxygen tanks.
175
176 **2.2. MES system**
177 In the *OxyMES* scheme, the inlet flows to the *MES* system are the combustion gases
178 produced in the oxyboiler (OxyFG), the make-up water for the *MES* cell, and the electricity
179 to maintain the potential between the electrodes, which will come from the RES surpluses.
180 The oxycombustion gases are flue gases from the combustion of the fuel with pure oxygen
181 and recycled flue gases. They are mainly composed of CO_2, water vapour, and N_2. The
182 product outlet streams of the *MES* cell are a high purity oxygen stream produced in the
183 anodic chamber and a biogas stream with a methane concentration above 50% by weight
184 leaving the cathodic chamber. Part of the oxygen produced in the *MES* cell is introduced
185 into the oxyboiler to perform oxycombustion and replace the ASU's oxygen supply. The
186 remaining oxygen is stored in a dedicated tank.
187 *MES* systems, designed from the perspective of *power-to-gas bioelectrochemistry*
188 (BEP2G), combine the production of energy carriers (CH_4) with the sequestration of CO_2
189 [30]. The model that simulates what happens inside the *MES* cell considers that the oxygen
190 evolution reaction (OER) that generates molecular oxygen (O_2) takes place at the anode.
191 Meanwhile, in the cathode, CO_2 is reduced to organic compounds due to the catalytic
192 action of microorganisms. The protons (H^+) cross the membrane separating the two half-
193 cells from the anodic chamber to the cathodic chamber. The redox half-reactions are as
194 follows:
195

Anode half-reaction

$2H_2O \rightarrow O_2 + 4e^- + 4H^+$ E^0 = -1.23 V (E^0 vs. NHE at pH 0) [Eq. 2]

Biocathode half-reaction

$CO_2 + 8H^+ + 8e^- \rightarrow CH_4 + 2H_2O$ E^0 = 0.169 V (E^0 vs. NHE at pH 0) [Eq. 3]

where E^0 are the standard potentials related to CO_2 reduction and water oxidation with reference to the Normal Hydrogen Electrode (NHE) at pH=0.

The process requires the contribution of energy from an external source, in the form of electrical energy, through the application of a potential to the electrodes that is sufficient to trigger the reduction–oxidation reactions (redox) and overcome the losses of the process. This external energy will come from the surpluses of the electrical system. One of latest published works on *MES* cells with simultaneous oxygen and methane production reports using a cell in which the potential applied between anode and cathode is 2.8 V [17]. It is noted that there are studies which have shown that microorganisms are still active after an electricity supply interruption [31].

As seen in the redox half-reaction (Eq. 3), 8 moles of electrons are needed to reduce 1 mole of CO_2 to methane. This implies that the gas flow to be treated from the oxyboiler stream requires a higher number of electrons to transfer through the external electrical circuit of the electrochemical cell compared to what would be required to produce other compounds such as hydrogen (supplementary material). Both the redox potential of the electrode and the pH of the electrolyte influence the species obtained in the cell [12].

Regarding electrode potentials, Villano et al. [14] observed that methane was produced at cathodic potentials more negative than −0.7 V (vs. Ag/AgCl), which corresponds to −0.5 vs. SHE at pH 7. At −0.8 vs. SHE, the efficiency of the conversion of electrical current into methane reached 96%. Later, Villano et al. [32] reported methane production of 9.7 ± 0.6 mmol/l day in a two-chamber *MEC* cell with a conversion efficiency of electrical current to

methane of 84-90% and a conversion efficiency of acetate to current at the anode of 72-80%. In most studies, the cathodic efficiency of methane production reaches 95-99% with biocathode potentials between -0.7 V and -0.8 V vs. SHE [12]. Similarly, Batlle-Vilanova [33] reported a biocathode potential of -0.8 V vs. SHE. They obtained a Faradaic conversion of 89.7% and a conversion ratio of CO_2 to methane of 95.8%. Recently, Gómez et al. [17] demonstrated the continuous production of methane in a cell, with and without a membrane, with a cathode potential between -0.9 V and 0.7 V vs. NHE, with an average cathodic efficiency of 84%.

During microbial electrosynthesis, a certain amount of thermal energy is produced in the cell. Potentially, this energy can be used in another part of the process if a heat-exchanger net is properly installed. In this study, the heat generated was considered to be negligible.

2.3. Integrated process. Balance of Plant (BOP)

Figure 3 identifies the main streams of the study. The gas stream to be introduced into the *MES* cell is taken from the outlet of the dust particle filter of the oxycombustion plant, normally set at 180 °C. At this point, the flue gases have the composition shown in Table 1. The flow and composition values of the fuel and the flue gases leaving the oxycombustion plant are obtained from the experimental tests performed in the reference demonstration plant [28], Table 1. The methodology followed was to model the process by performing the mass and energy balances of each of the process streams.

Table 1. *Flue gases composition at oxyboiler plant outlet and MES cell inlet; biogas composition at MES cell outlet.*

	Oxy-Flue Gas, oxyboiler outlet	Oxy-Flue Gas, MES cell inlet	Biogas, MES cell outlet

	(%w_{th}, w.b.)	(%w_{th}, w.b.)	(%w_{th}, w.b.)
CH_4	-	-	57.96
CO_2	73.79	82.06	8.39
H_2O	10.38	2.91	2.91
N_2	11.56	12.86	26.29
O_2	3.54	1.57	3.22
SO_2	0.33	0.15	0.30
Ar	0.40	0.45	0.92

In this study, a base case of oxyboiler operation is considered, that is, feeding 2550 kg/h of bituminous coal with the characteristics shown in supplementary material. This operational scenario remains fixed for the entire study, so the flow rate of oxycombustion gases entering the *MES* cell is also constant and, therefore, the biogas produced, for all cases.

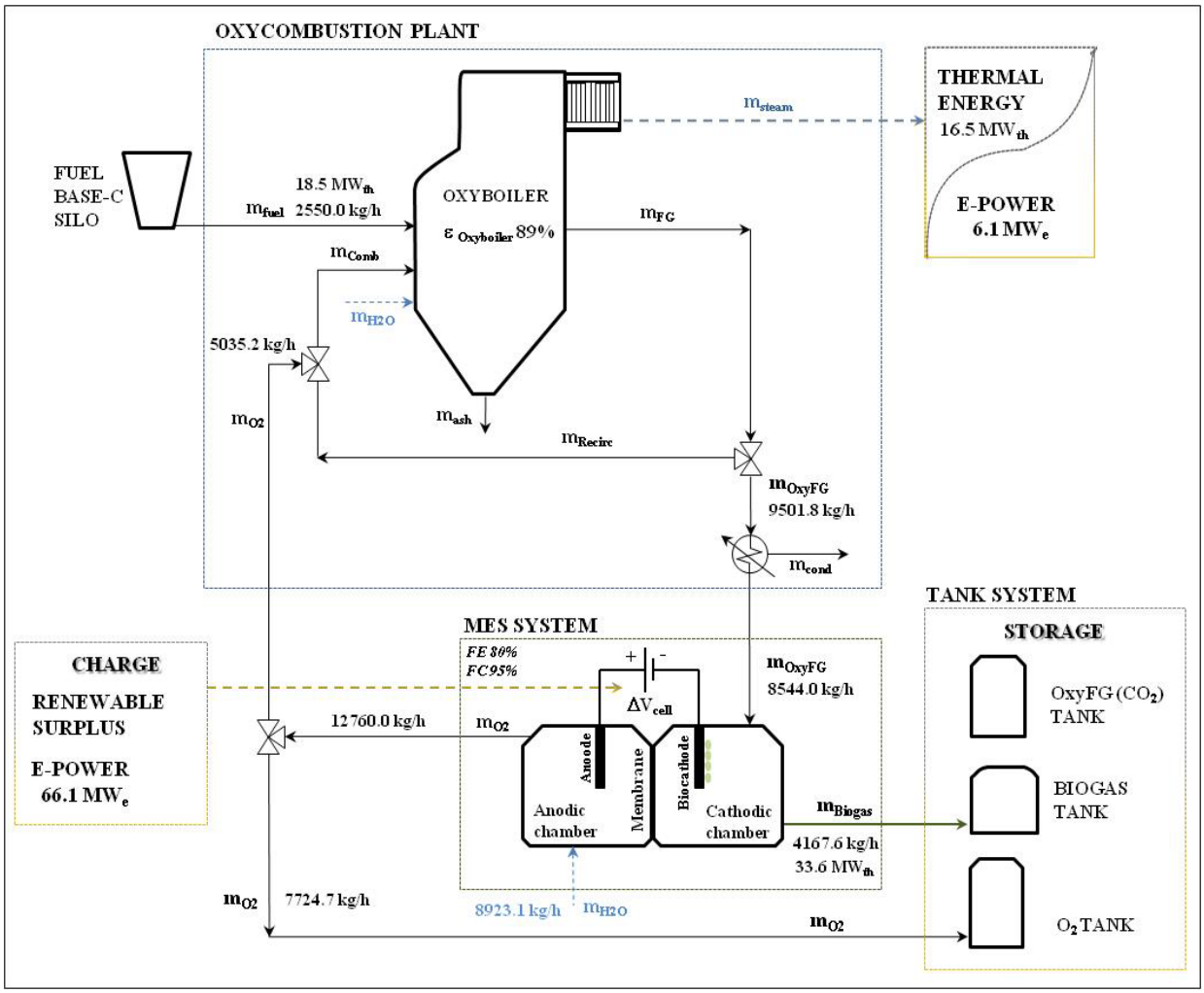

***Fig. 3**. Conceptual layout of the analysed OxyMES system, including main mass and energy flow data.*

To avoid affecting the microorganisms of the *MES* cell, the temperature of the gas stream is set at 32 °C [34]. In addition, since the process must be anaerobic, the oxygen content in the flue gas stream is limited to a maximum of 2% by volume. However, there are recent studies that indicate the possibility of reaching higher values, although methane production is reduced [35]. Keeping oxygen below $2\%_{vol}$ involves incorporating a gas conditioning train ahead of the cell for cooling and condensing its moisture as well as part of the SO_2 and O_2 content. In practice, if the oxygen content requirement is not met, then dedicated equipment (deOxo or similar) should be included to ensure this condition (out of the scope

of this work). According to calculations, the biogas generated in the *MES* cell has the composition shown in Table 1.

***Table 2**. Main technical characteristics for units and subunits. Simulation assumptions and operational parameters for sizing the main units of the OxyMES system.*

Oxyboiler plant inlet/outlet	MES cell inlet/outlet
Fuel (pulverized coal) flow, m_f: 2.55 t/h	Oxycombustion flue gases flow: 8.5 t/h **
LHV_{fuel}: 26137 kJ/kg	CO_2 flow (contained in the oxy-flue gases): 7.0 t/h
Input thermal power, LHV, P_{in}: 18.5 MW_{th}	O_2 content in oxy-flue gas: < 2%$_{vol}$
Oxyboiler thermal efficiency, LHV, $\mu_{oxyboiler}$: 89%	Net water consumption: 8.9 t/h
Output thermal power, LHV, P_{out} (Q_b): 16.5 MW_{th}	Electrical power consumption: 66.1 MWe ***
Oxygen flow (fresh): 5.0 t/h	Biogas flow, m_{Biogas}: 4.17 t/h
Oxycombustion flue gases flow: 9.5 t/h ;180 °C *	CH_4 flow (contained in biogas), m_{CH4}: 2.4 t/h
	LHV_{CH4}: 50000 kJ/kg
	Biogas power, LHV: 33.64 MW
	Faradaic efficiency, FE: 80%
	CO_2-to-methane conversion rate, FC: 95%
	Operational temperature: 30-35 ° C

* *Oxycombustion flue gases at oxyboiler plant outlet, after recirculation (before stack).*

** *Oxycombustion flue gases after water condensation, at MES cell inlet.*

*** *The electrical power input for the MES is* calculated considering ΔV_{cell}:1.63 V, FE: 80%; FC: 95%.

The chemical energy stored by the *OxyMES* is a function of the operating hours of the aforementioned system and these, in turn, are a function of the storage tank capacity for the biogas produced in the *MES* cell. The design assumes that the operation hours will correspond to the number of hours in which the renewable electricity surpluses are produced, although this is a criterion that can vary according to the final application and the degree of autonomy sought. In this case, the hypothesis of 10 hours of *MES* cell

operation was considered. With this assumption, the chemical energy stored as biogas is 336 MWh_{th}. In turn, the operation of the oxyboiler is directly conditioned by the capacity of the oxygen tank, since this must be sufficient to cover the hours that the plant is in operation. The system of tanks for the storage of process fluids is a key element that directly affects the operation of the whole plant, and it must be properly designed so that it can meet the expected stored energy (MWh) and autonomy objectives of the plant.

The *OxyMES* system can be parameterized as an energy storage system: 33.6 MW/336 MWh. Without going into detailed considerations, the capacity and autonomy of the CO_2 tank are the parameters that will define the maximum power of the *OxyMES* system (33.6 MW), while the capacity of the biogas tank indicates the stored energy (336 MWh).

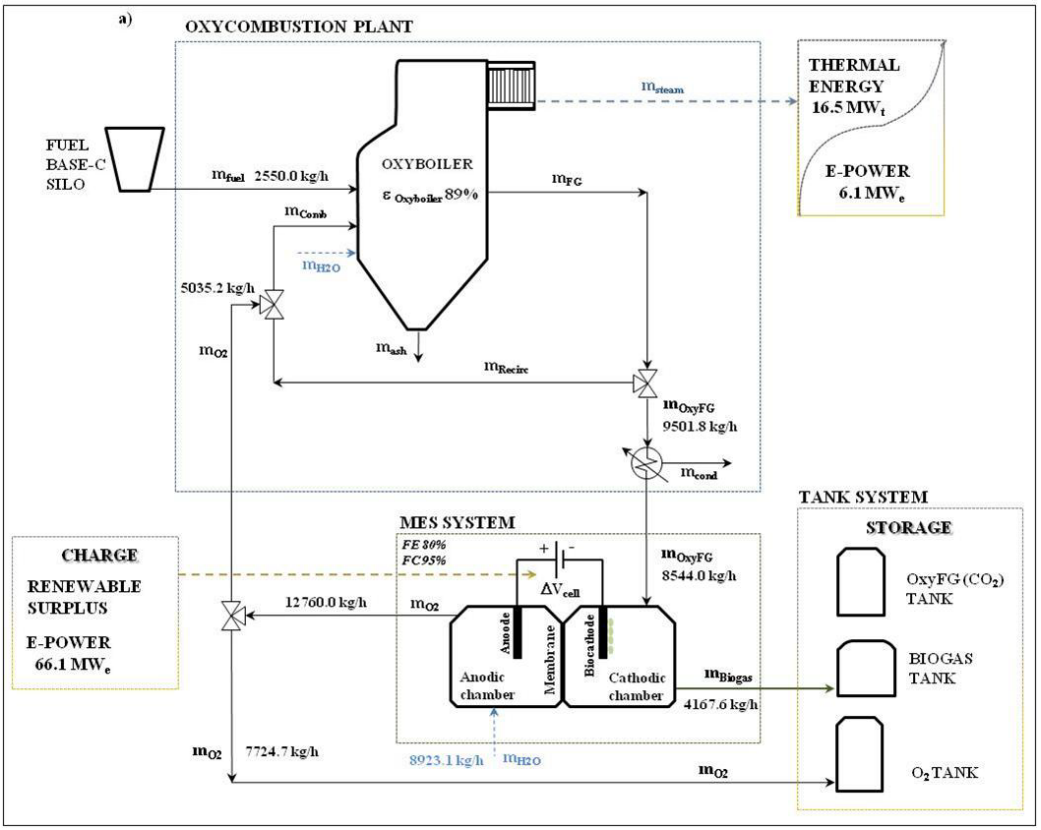

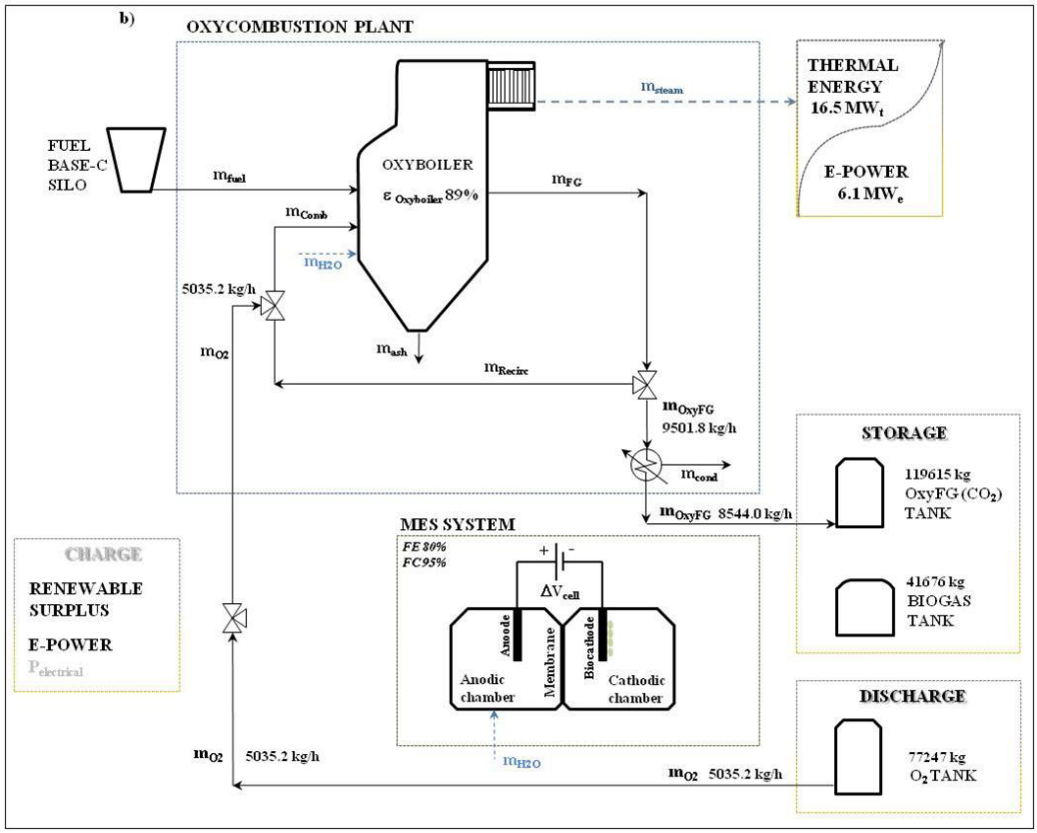

286

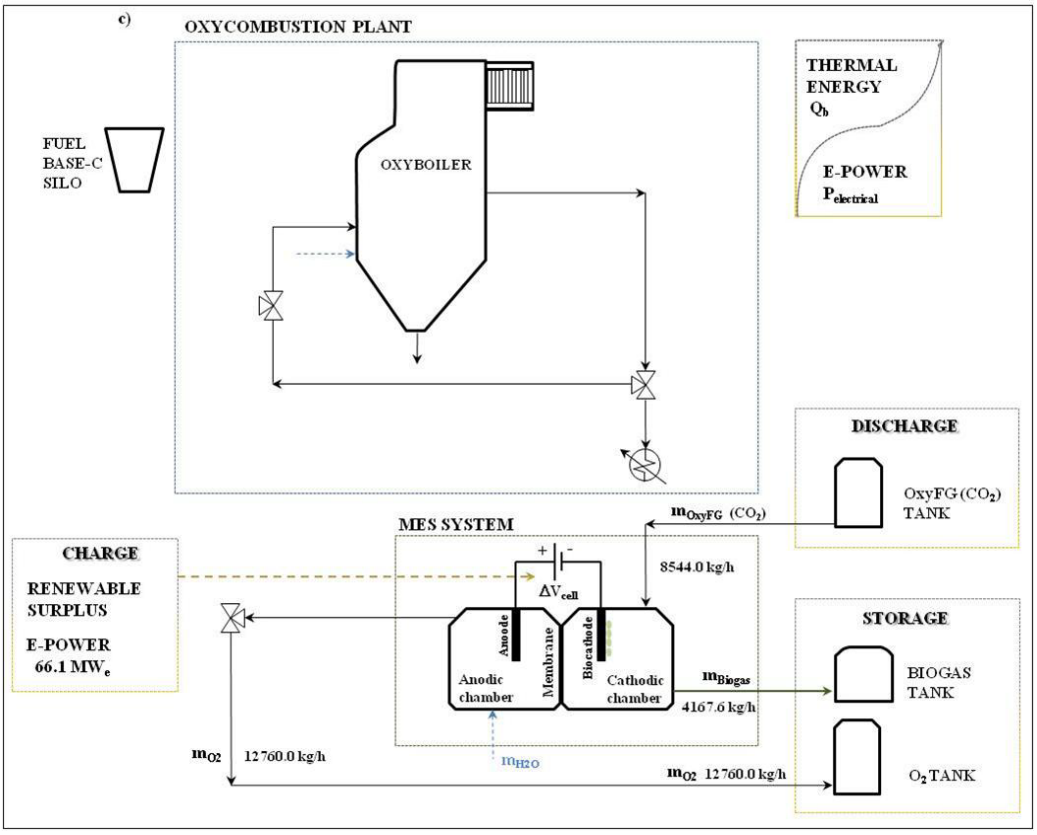

287

288 ***Fig. 4****. Charge, discharge, and storage cycles in the OxyMES system standard operation profile. a)*

289 *Oxyboiler and MES are ON: CO_2 from oxyboiler is fed to the MES cell, and it is converted to biogas and*

stored during an RES surplus period (RES charge, biogas and O_2 storage). b) Oxyboiler ON and MES OFF: CO_2 from oxyboiler is led to its storage tank during high-demand periods with no RES surplus; O_2 is fed to the oxyboiler to maintain the oxycombustion (CO_2 charge, O_2 discharge). c) Oxyboiler OFF and MES ON: during oxyboiler shutdowns when RES surplus occurs, CO_2 from the tank is fed to the MES cell to convert it into biogas (RES charge, CO_2 discharge, biogas and O_2 storage).

To size the complete *OxyMES* system, first, a daily operating profile of the *MES* cell is defined, considering that it operates during the hours in which the RES surpluses occur. For this work, an average of 10 h per day concentrated in the central hours of the was been considered [36]. This assumption was made by analysing the expected *oversupply* of renewable energy in the scenarios projected to 2030 with a high penetration of renewable energy (mainly solar and wind) and without storage systems (Fig. 5). It is during the operation of the *MES* cell that the biogas produced and the oxygen left unconsumed in the oxyboiler will be stored. Therefore, the oxygen stored during the charging process (Fig. 4.a) must be sufficient to cover the oxygen consumption of the oxyboiler during the next period in which the *MES* cell is no longer coupled to the oxyboiler because there is no surplus of renewables (Fig. 4.b). The final capacity of the tank system will depend on the hourly, daily, or even weekly scope defined by the operator of the industry or, in other words, the stored energy (MWh) that is to be made available to the system.

***Table 3**. Hourly flows of CO_2 consumed and oxygen and biogas produced in the MES cell from the mass balance calculations.*

MES cell, inlets streams (consumptions)	
Oxyboiler flue gas flow after cooling, kg/h	8544
CO_2 flow (contained in the oxy-flue gas) after cooling, kg/h	7011
Net water flow, kg/h	8923
(RES) Electrical power, MWe	66

MES cell outlets streams (products)	
Raw biogas flow, kg/h	4178
Methane flow (contained in the biogas flow), kg/h	2422
Oxygen flow, kg/h	12760

312

313 ***Table 4***. *Minimum capacity of CO_2, O_2, and biogas tanks for 10 hours of MES cell operation. * Note: biogas*

314 *is stored after a deSOx treatment (Fig. 3).*

MES cell, 10-hour operation profile	
Biogas stored*, kg//tank autonomy, h	41676//10 h
Biogas chemical energy stored, MWh_{th}	579
Oxygen stored, kg//tank autonomy, h	77247//10 h
Net oxygen stored (stock), kg	6754
CO_2 stored, kg//tank autonomy, h	119615//14 h

315

316

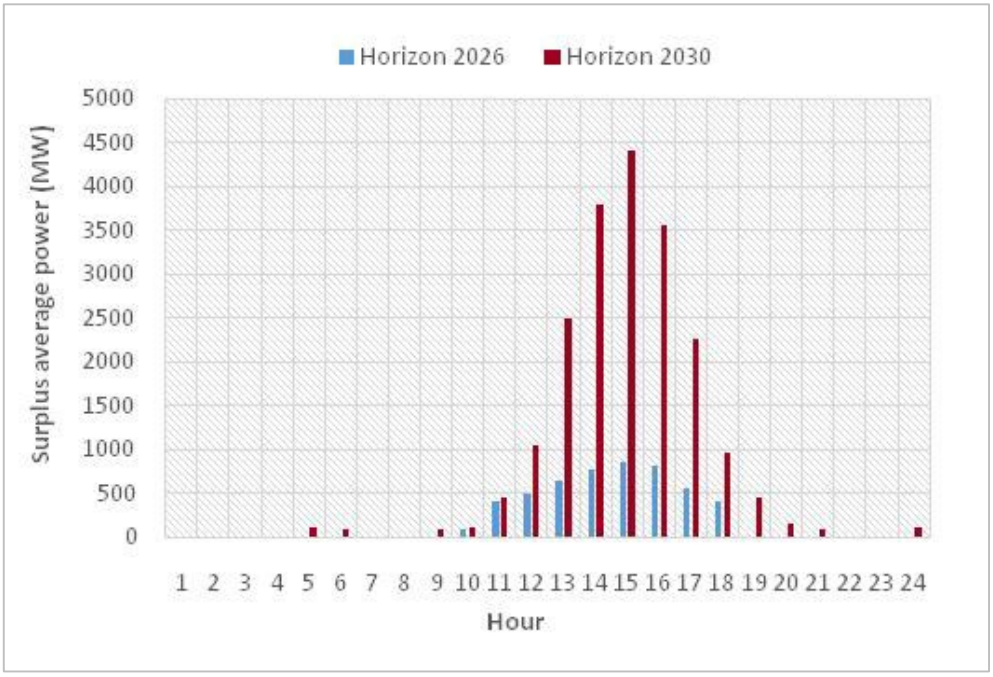

317

318 ***Fig.5***. *Pattern of hourly oversupply associated with photovoltaic (PV) production in Spain (central hours of*

319 *the day). In 2030, it will be able to reach values above 4000 MW. Adapted from* [37].

320

2.4. Analysis of partial performance and global performance of the OxyMES hybrid process

To evaluate the *OxyMES* process, the efficiency of the two main subsystems (oxyboiler and *MES* cell) that make up the hybrid system have been defined. These performances are calculated by the relationship between the energy produced and the energy supplied to operate the subsystem according to their respective boundary limits (dashed lines in Fig. 3). Then, the global *OxyMES* system performance can be obtained.

The thermal energy generated in the oxyboiler Q_b (MW_{th}) is a function of the performance of the oxycombustion boiler, $\eta_{oxyboiler}$, which was calculated from the experimental data gathered in [29], resulting in an average value of 89% LHV basis, which is close to that reported in various studies on oxyfuel power plants (> 87.37% HHV, [26]; > 90% - 93% LHV, [38]). This Q_b is the thermal energy of the steam produced, and it is available for thermal uses of the plant or for its conversion to electrical energy through a Rankine cycle in a steam turbine.

$$\eta_{\text{Oxyboiler, LHV basis}}(\%)=\frac{Qb_{\text{Oxyboiler}}}{LHV_f \cdot m_f} x100 \qquad \text{[Eq. 4]}$$

In relation to the *MES* system, the electrical energy consumed comes from the *RES* surplus of the network. This is used to maintain the potential in the electrodes of the electrochemical cell, which is necessary to promote the transport of electrons that convert the CO_2 molecules into CH_4. In turn, the chemical energy of the methane produced in the biocathode, E_{Biogas}, can be considered to be energy produced by the *MES* cell. The **electrical energy consumed** in the *MES* cell, required to reduce the CO_2 to methane, is shown in Eq. 5:

$$E_{MES}=\Delta V_{cell} \cdot I \qquad [MJ/tCH_4] \qquad \text{[Eq. 5]}$$

where ΔV_{cell} is the external voltage applied to the cell, and I is the current intensity calculated as the specific flow of electrons from the anode to the cathode through the external electrical circuit.

$$\Delta V_{cell} = \Delta V_{theoretical\ cell} + E_{overpotentials} = E^0_{cathode} - E^0_{anode} + E_{overpotentials}\ [V] \quad [Eq.\ 6]$$

Due to the losses of the electrochemical process in both electrodes, $E_{overpotential}$, it is necessary to apply a ΔV_{cell} potential greater than that theoretically necessary according to the thermodynamics of the global redox reaction, with $\Delta V_{theoretical\ cell} = E^0_{cathode} - E^0_{anode} =$ 0.169 - (- 1.23) = -1.06 V vs. NHE, pH 0 [Eq. 7], where E^0 values are the standard potentials of the electrodes. The negative sign indicates that the reaction is not spontaneous.

To obtain the efficiency of the global microbial electrosynthesis process, the actual conversion of CO_2 to methane (FC or CO_2-to-CH_4 ratio) must be considered, thus expressing the carbon captured and converted into product. It is also necessary to consider the faradaic efficiency, FE, which is a factor that indicates the efficiency in the electrical conversion towards that product in the electrodes of the cell (mainly, cathode) [33]. With these parameters, the specific flow of electrons per ton of methane produced, I, is calculated (Fig. 1):

$$I = n_{CH4} \cdot n_{e^-} \cdot F \cdot 100/FE \quad [C/tCH_4] \quad [Eq.\ 8]$$

where n_{CH4} indicates the moles of the product, CH_4/tCH_4, n_{e^-} indicates the moles of electrons per mole of CO_2-to-CH_4, and F is the Faraday constant, 96485 C/mol e^-.

The electrical power consumed by the *MES* cell is shown in Eq. 9,

$$P_{e\_MES} = E_{MES} \cdot m_{CH4} \quad [MW] \quad [Eq.\ 9]$$

where m_{CH4} is the methane flow rate in t/h produced in the *MES* cell. The supplementary material includes the development of the calculation to obtain the specific current intensity, I, and the electrical consumption E_{MES} in the MES cell.

In experimental studies, it was found that to achieve promising results in the cell operating parameters, the potential applied (ΔV_{cell}) should vary, in practice, between values close to 4 V [39] and 2.6 V [17] It is expected that these values can be reduced to approximately 1.7 V, in view of the lower value of biocathode potential reported (-0.4 V vs. SHE) by Beese-Vasbender et al. [40], who also reached a cathodic efficiency of 80%.

Based on the bibliographic references, [12] and [17], a Faradaic efficiency value, FE, of 80% and a CO_2 to methane conversion factor, FC, of 95% were used for the calculation of the electrical consumption of the *MES* cell in this study. Applying the previous equations, the results of the electrical power consumed, $P_{e\_MES,}$ are presented in Table 5 for four assumptions of the external applied voltage (ΔV_{cell} = 1.23 V, 1.63 V, 2.8 V, and 3.5 V).

With all of the above, the energy efficiency of the *power-to*-gas conversion is calculated in the *MES* cell (η_{PtG_MES}) as the ratio between the power obtained in the form of chemical energy from biogas (P_{Biogas}) and the electrical power supplied to produce the aforementioned biogas (P_{e_MES}):

$$\eta_{PtG_{MES}}(\%)=\frac{P_{Biogas}}{Pe_{\_MES}}x100=\frac{LHV_{CH4}\cdot m_{CH4}}{\Delta Vcell\cdot I\cdot m_{CH4}}x100 \qquad \text{[Eq 10]}$$

The value obtained from this *power-to*-gas efficiency, η_{PtG_MES}, for the case ΔV_{cell} = 1.63 V is 50.88%, as shown in Table 5.

Finally, once the energy balances are performed for each subunit, the **overall efficiency of the OxyMES process** is calculated (η_{PtGtH_OxyMES}) taking as inputs to the boundaries of the global system, the chemical power contained in the oxyboiler fuel ($LHV_f \cdot m_f$) and the electrical power that feeds the *MES* cell (P_{e_MES}) and, as outputs, the thermal power of the steam produced in the oxyboiler ($Q_{bOxyBoiler}$) and the chemical power of the biogas (P_{Biogas}) generated in the biocathode of the *MES* cell:

$$\eta_{PtGtH\_OxyMES}(\%)=\frac{Q_{b\ OxyBoiler}+P_{Biogas}}{LHV_f m_f+P_{e\_MES}}x100=\frac{Q_{b\ OxyBoiler}+LHV_{CH4}\cdot m_{CH4}}{LHV_f m_f+\Delta Vcell\cdot I\cdot m_{CH4}}x100 \qquad \text{[Eq. 11]}$$

If the global performance is calculated for the selected base case of the oxyboiler operation (18.51 MW_{th} LHV, Table 5, corresponding to the 2550 kg/h of bituminous coal selected) and an external potential of ΔV_{cell} = 1.63 V is modelled in the MES cell, the result obtained is 59.22%, Table 5.

3. RESULTS AND DISCUSSION

The tank system allows the transfer of energy in the successive cycles of charging and discharging to/from the electrical and gas system with oxygen acting as *feedstock* and biogas as an *energy carrier*. Regarding the operating profile, to carry out these charging and discharging cycles, the oxygen and biogas tanks are sized so that they can cover the demand of the boiler during the periods in which the *MES* cell is inactive. In these periods (Fig. 6, 12 am-8 am and 7 pm-12 pm), the oxycombustion gas stream is stored in its corresponding tank (Fig. 4.b). Table 4 shows the minimum tank capacities for 10-hours of continuous cell operation. However, the final sizing of the tank system will be determined not only by the duration of the product charging and discharging cycles but also by its operation profile (continuous/discontinuous) and by the planning of its final discharge in each cycle of plant operation. In this study, the *cycle of operation* of the plant is defined as the time between the discharges of the accumulated oxygen, CO_2, and biogas stock to the external network.

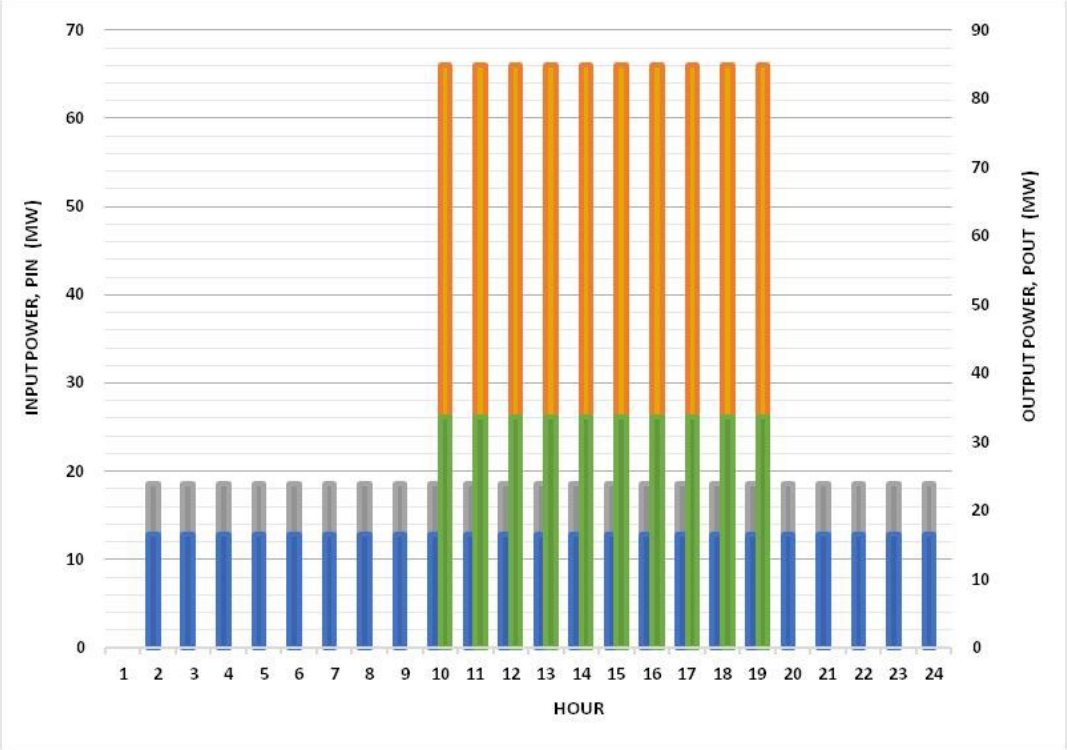

412

413 ***Fig. 6***. *OxyMES daily operation profile adjusted to the RES discharge profile in Spain.* $P_{in\ TOT}$ *(blue) refers to*
414 *the total power input (MW) to the global system per hour: sum of chemical coal-fuelled power consumed by*
415 *the oxyboiler (grey) and electric power consumed by the MES cell (yellow).* $P_{out\ TOT}$ *refers to the total power*
416 *produced (MW) by the global system per hour: sum of steam heat power (MW) generated in the oxyboiler*
417 *(dark blue) and biogas chemical power produced (MW) by the MES cell (green).*

418

419 Fig. 7 shows the influence of the operating profile of the plant on the number and size of
420 the final tanks to be installed. If the discharge cycle is a daily one, the size of the oxygen
421 storage tank can be optimized by proposing a discontinuous intraday cell operation, Fig. 8.
422 The greater the time lag between the two start-ups of the *MES* cell, the lower the required
423 maximum value of the oxygen tank capacity.

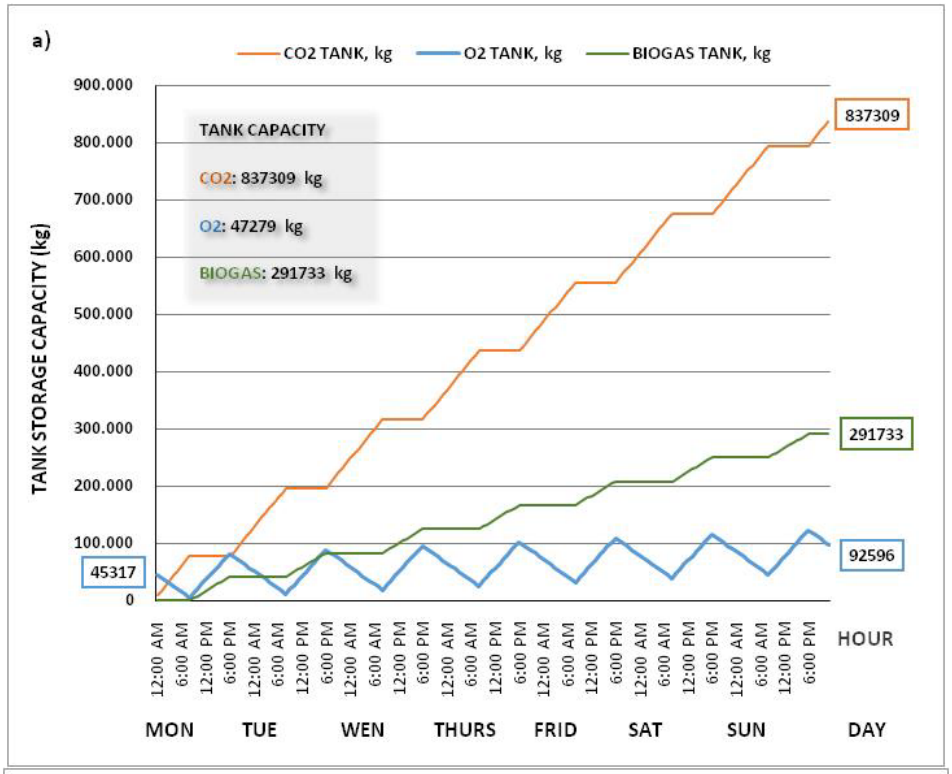

424

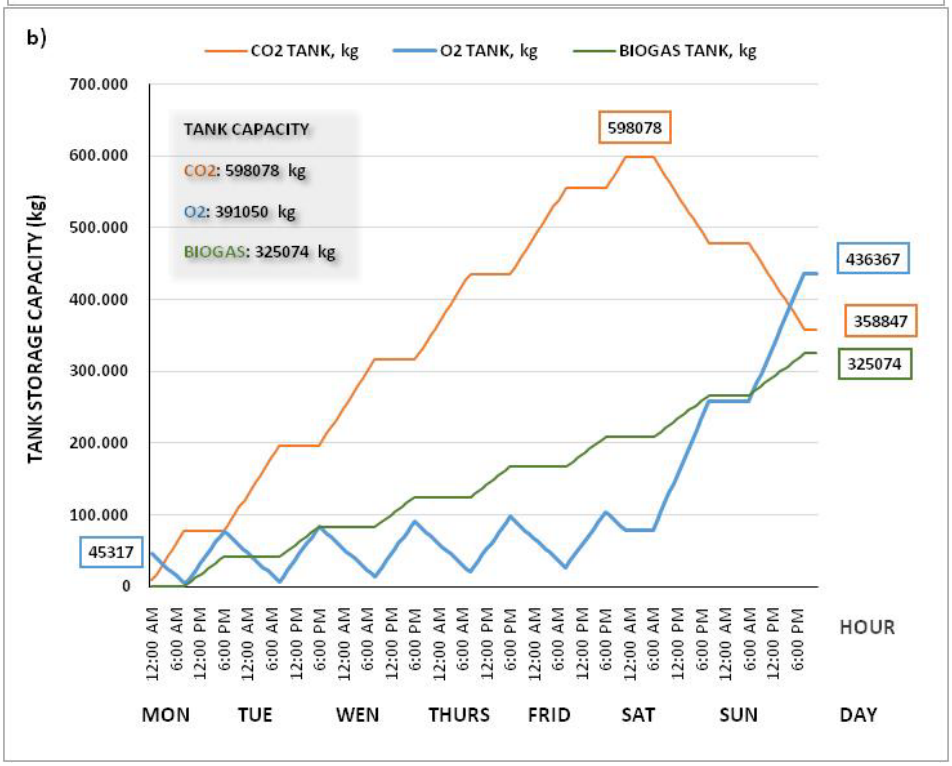

425

426 ***Fig. 7 a, b***. *Daily operation of the OxyMES system in the weekly operation cycle: a) Continuous operation*
427 *from Monday to Sunday, 24 h/day for oxyboiler and 10 h/day for MES cell; b) Continuous operation from*
428 *Monday to Friday, 24 h/day for oxyboiler and 10 h/day for MES cell; from Saturday to Sunday, 14 h/day for*
429 *MES cell (assuming higher surplus hours during the weekend). In each operation scenario a) and b), the*

minimum weekly storage capacity necessary for the CO_2, O_2, and biogas tanks is obtained according to the plant operation cycle.

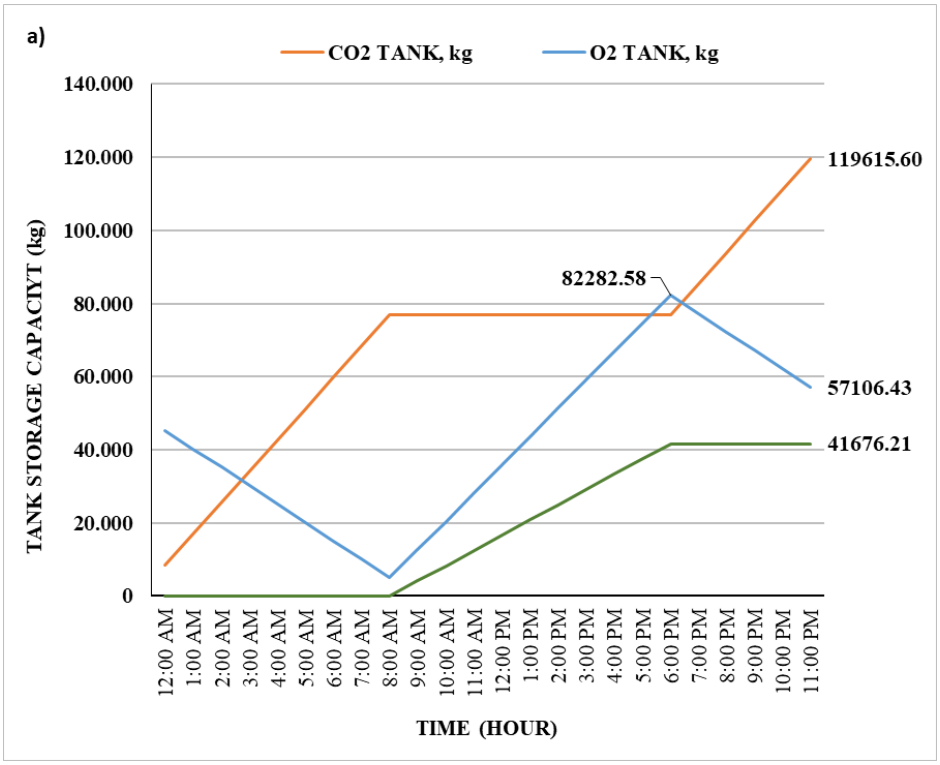

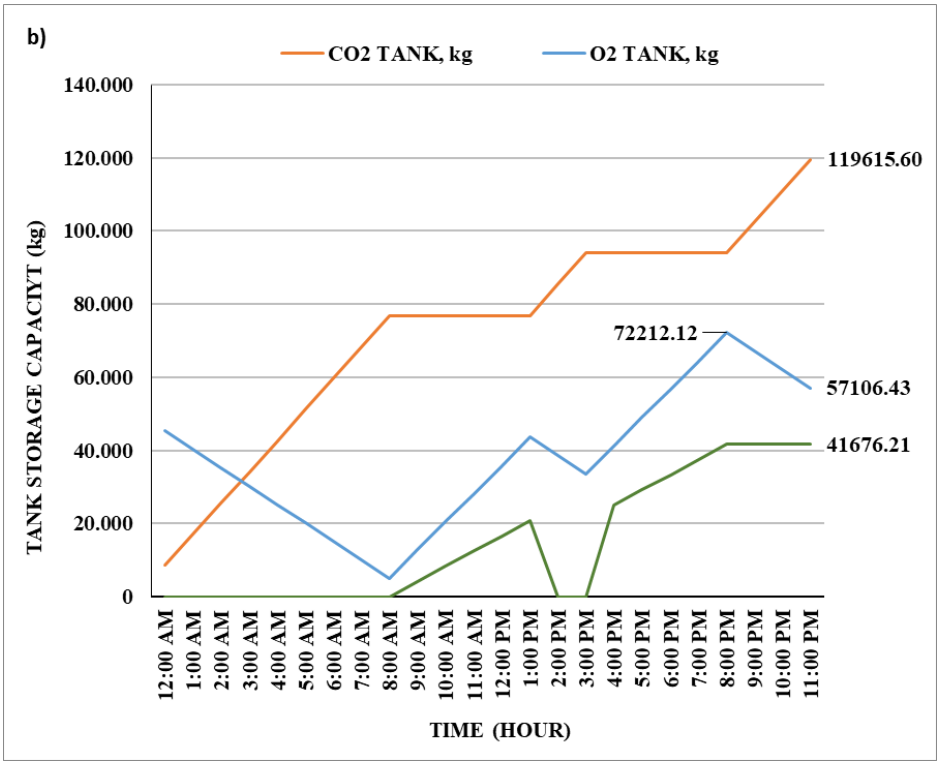

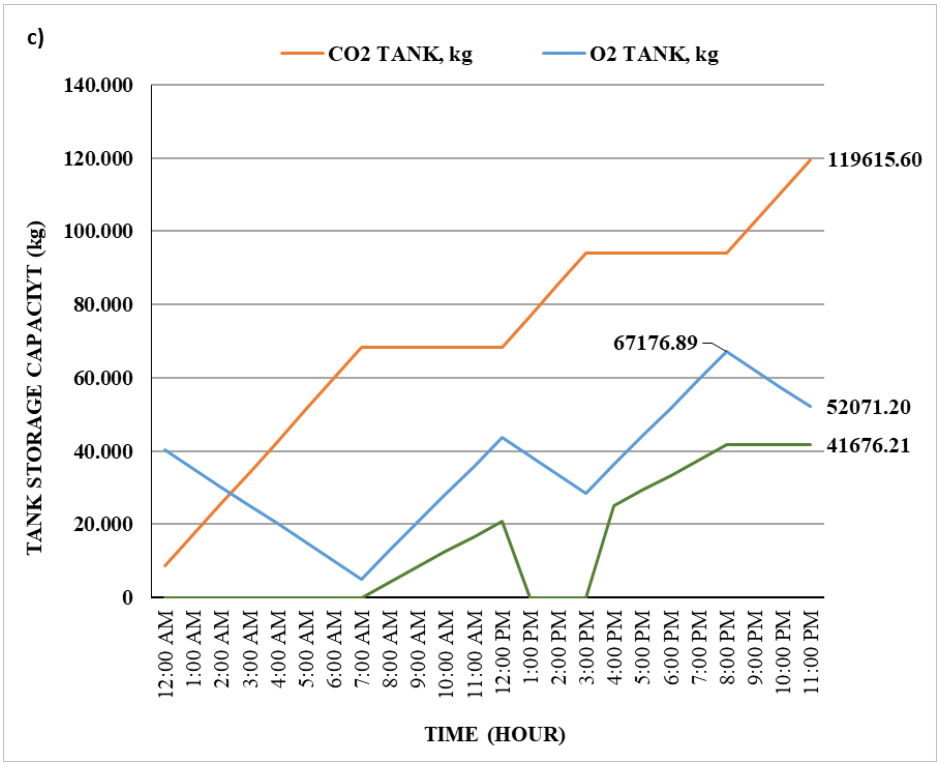

436

437 ***Fig. 8 a, b, c****. Tank storage capacity operating with a daily discharge cycle: a) continuous operation of 10*
438 *hours of MES cell; b) discontinuous operation in two 5-hour periods of MES cell with two hours of lag*
439 *between each period; c) discontinuous operation in two 5-hour periods of MES cell with three hours of lag*
440 *between each period. The peak capacity value of the oxygen tank decreases as the offline period of the MES*
441 *cell increases between operating periods.*

442

443 From an application perspective in new decentralized energy models, the difference in
444 storage capacity results obtained under flexible operating profiles (Fig. 8) seems to indicate
445 that the *OxyMES* schemes will better optimize their design and operation if they are
446 integrated into local networks connecting various industries, forming an *industrial hub*, so
447 that they can transfer their surplus energy *pre-carriers* and *carriers* (CO_2, oxygen, and
448 biogas). The interconnection network itself will act as a buffer of the whole system, and
449 this would be a matter of advancing the construction of a "*system of systems*" aimed at the
450 effective implementation of circular and sustainable economy models [41].

451

3.1. Comparison of efficiency according to different scenarios of *MES* cells

For the same biogas production, four scenarios have been proposed in the sensitivity analysis of the efficiencies μ_{PtGtH_OxyMES} as a function of the cell potential (ΔV_{cell}) which is directly related to the energy consumed by the cell (Table 5). The four scenarios analysed are based on data and initial assumptions reported by different research groups mentioned throughout the article. These scenarios seek to cover a reasonable range of *MES* cell operation in terms of the external potential to be applied. The most unfavourable potentials selected for the study are those that assume a greater electrical consumption in the cell, ΔV_{cell} = 3.5 V, a case similar to that reported by Zhou et al. [39] and ΔV_{cell} = 2.8 V by Gomez et al. [17], and these represent the current state of the art (TRL3-4).

On the other hand, an optimistic scenario is proposed with lower cell overpotentials. According to the trend in the results obtained by the different research teams, it is predicted that this optimistic scenario can be achieved in the short term. In this case, the applied voltage would be ΔV_{cell} = 1.63 V, and this assumption was reached based on the lowest biocathode potential reported by Beese-Vasbender et al. [40] (-0.4 V vs. SHE). Finally, the fourth scenario simulates the theoretical minimum cell potential to be applied (ΔV_{cell} = $\Delta V_{theoretical\ cell}$ = 1.23 V) when considering no overpotential losses. This scenario would represent the theoretical upper limit of the performance value that *OxyMES* could aim for. In all scenarios, the same flow of oxycombustion gases entering into the *MES* cell is considered.

476 ***Table 5***. *Summary of energy produced and consumed and the efficiencies obtained for four* ΔV_{cell}
477 *scenarios.*

	ΔV_{cell} = 1.23 V	ΔV_{cell} = 1.63 V	ΔV_{cell} = 2.8 V	ΔV_{cell} = 3.5 V
Chemical power of inlet fuel fed to oxyboiler (LHV), MW_{th}	18.51	18.51	18.51	18.51
$\eta_{Oxyboiler}$, Oxyboiler efficiency (LHV), %	89.00	89.00	89.00	89.00
Q_b, heat absorbed by steam, MW_{th}	16.48	16.48	16.48	16.48
Chemical power of biogas (LHV), MW_{th}	33.64	33.64	33.64	33.64
P_{e_MES}, *MES* electric consumption, MW_e	**49.89**	**66.11**	**113.57**	**141.96**
η_{PtG_MES} *MES* efficiency, %	**67.43**	**50.88**	**29.62**	**23.70**
η_{PtGtH_OxyMES}, *OxyMES* overall efficiency, %	**73.26**	**59.22**	**37.94**	**31.23**

478

479 Table 5 shows the influence of the electrical cell overpotentials on the performance [42].
480 This influence is due to their direct relationship with the *MES* cell electrical consumption.
481 Reducing these losses to a minimum is a fundamental objective to advance the
482 development of *MES* technologies and their integration into different processes. The results
483 obtained indicate achievable values of *power-to-gas* performance (η_{PtG_MES}) of 51% in the
484 *MES* cell and 60% for the *OxyMES* integrated overall system (η_{PtGtH_OxyMES}).
485 These data agree with those reported for other *power-to-gas* schemes with electrolysers
486 and methanation reactors. Thema et al. [43] reported real efficiencies of around 41%,
487 which is low compared to theoretical values of 49–79% (with the use of heat). Frank et al.
488 [44] calculated a range between 50-80% and 33-53% for the best and worst cases,
489 depending on the use of heat. Bailera et al. [20, 21] included utilization of the synthetic gas
490 to produce power in a combined cycle with efficiencies of power to gas and oxyfuel
491 combustion between 55% and 60% (depending on electrolyser specific consumption) and

492 56% for electricity to synthetic natural gas. This comparison highlights the significance of
493 the proposed scheme in opening a new and interesting research topic.
494
495 **3.2. Comparison of *OxyMES* with conventional CO_2 capture plants**
496 Another interesting advantage of the *OxyMES* process is that the production of the oxygen
497 necessary for the oxycombustion is carried out '*in situ*' in the *MES* reactor. This represents
498 a significant advantage in that it avoids the CAPEX and the OPEX of the oxygen
499 generation units used in conventional oxycombustion plants with CO_2 capture (ASU) [45].
500 The ASU facilities assume between 5% and 6% penalties in the global energy efficiency of
501 an oxyfuel CO_2 capture plant [46]. Similarly, a CO_2 compression and purification unit
502 (CPU) is necessary for the delivery of the CO_2 captured for transport and deep geological
503 storage. In this case, the global efficiency penalty introduced by these units is between 4.5
504 % and 5% [38].
505 If we analyse the specific energy consumptions, W_{ASU} and W_{CPU} (kWh_e/kWh_{th}), of the
506 ASU and CPU facilities that no longer need to be installed in the *OxyMES* scheme,
507 expressed over the thermal energy of the steam produced in the oxyboiler, and compare
508 them to the new units that need to be installed, W_{MES} (*MES*), an approximate quantification
509 of the relative energetic improvement against an oxycombustion plant with conventional
510 CO_2 capture (see supplementary material) can be done. As a first option, storing the biogas
511 for subsequent delivery to the gas system is proposed. This would require prior treatment
512 for upgrading to biomethane. For the calculation of $W_{Upgrading}$ (kWh_e/kWh_{th}), the specific
513 energy consumption of the upgrading plant considered is 0.28 kWh_e/kg biogas (0.25
514 kWh_e/Nm^3 biogas) as reported in [47] for water scrubber and PSA technologies.
515 Table 6 shows the results of this comparative study which was carried out on the scenario
516 of ΔV_{cell} = 1.63 V. In option A, the specific energy consumption of the *MES* cell (W_{MES})

has been included, while this consumption is considered negligible in options B and C because it comes from surpluses of the electrical system. Option C reflects the improvement when the biogas is used as produced ($W_{Upgrading} = 0$).

[Energy saved ($\sum E_s$) + Energy produced ($\sum E_p$)] vs. [Energy consumed ($\sum E_c$)] [Eq. 12]

Table 6. Relative specific consumption: results from comparison with the reference plant (oxycombustion plant with CPU). Note: Options A1, B1, and C1 account for the biogas energy considering an electrical transformation in a small-size CCGT. Options A2, B2, and C2 refer to the worst scenario (no biogas energy is accounted for). W_{Biogas} was calculated considering a thermal to electric conversion efficiency of 36.43% (efficiency of a small-size CCGT plant). W_{ASU} was calculated considering 190 kWhe/tO_2 [20] and a W_{CPU} of 120 kWhe/CO_2 [48].

	W_{ASU} (E_s) (kWh$_e$/kWh$_t$ Q$_b$)	W_{CPU} (E_s) (kWh$_e$/kWh$_t$ Q$_b$)	W_{Biogas} (E_p) (kWh$_e$/kWh$_t$ Q$_b$)	W_{MES} (E_c) (kWh$_e$/kWh$_t$ Q$_b$)	$W_{Upgrading}$ (E_c) (kWh$_e$/kWh$_t$ Q$_b$)	ENERGY GAIN OR LOSS (kWh$_e$/kWh$_t$ Q$_b$)
IMPROVEMENT OPTION A: ASU & CPU avoided, *MES* and upgrading biomethane to network						
A.1	0.0581	0.0511	0.7437	4.01244	0.0712	-3.2308
A.2	0.0581	0.0511	0.0000	4.01244	0.0712	-3.9745
IMPROVEMENT OPTION B: ASU & CPU avoided, *MES* 100% surplus RES and upgrading biomethane to network						
B.1	0.0581	0.0511	0.7437	0.00000	0. 0712	0.7816
B.2	0.0581	0.0511	0.0000	0.00000	0. 0712	0.0379
IMPROVEMENT OPTION C: ASU & CPU avoided, *MES* 100% surplus RES, biogas for self-consumption						
C.1	0.0581	0.0511	0.7437	0.00000	0.00000	0.8528
C.2	0.0581	0.0511	0.0000	0.00000	0.00000	0.1091

The improvements obtained according to options B.1 and B.2 indicate that, depending on the chosen biogas upgrading technology [47], the avoided specific energy consumption of ASU and CPU (W_{ASU} and W_{CPU}) could alone compensate for the specific energy

consumption ($W_{Upgrading}$) of the upgraded installation, even without considering the biogas energy (option B.2). The best energy improvement is achieved when upgrading is not required (options C.1 and C.2), for example, when the raw biogas produced is utilized for self-consumption purposes which doesn't need to meet NG network quality. Further studies could address potential alternatives for this, such as coupling a combined cycle gas turbine power unit downstream of the *MES* cell or replacing the original fossil fuel of the oxyboiler, Fig. 9.

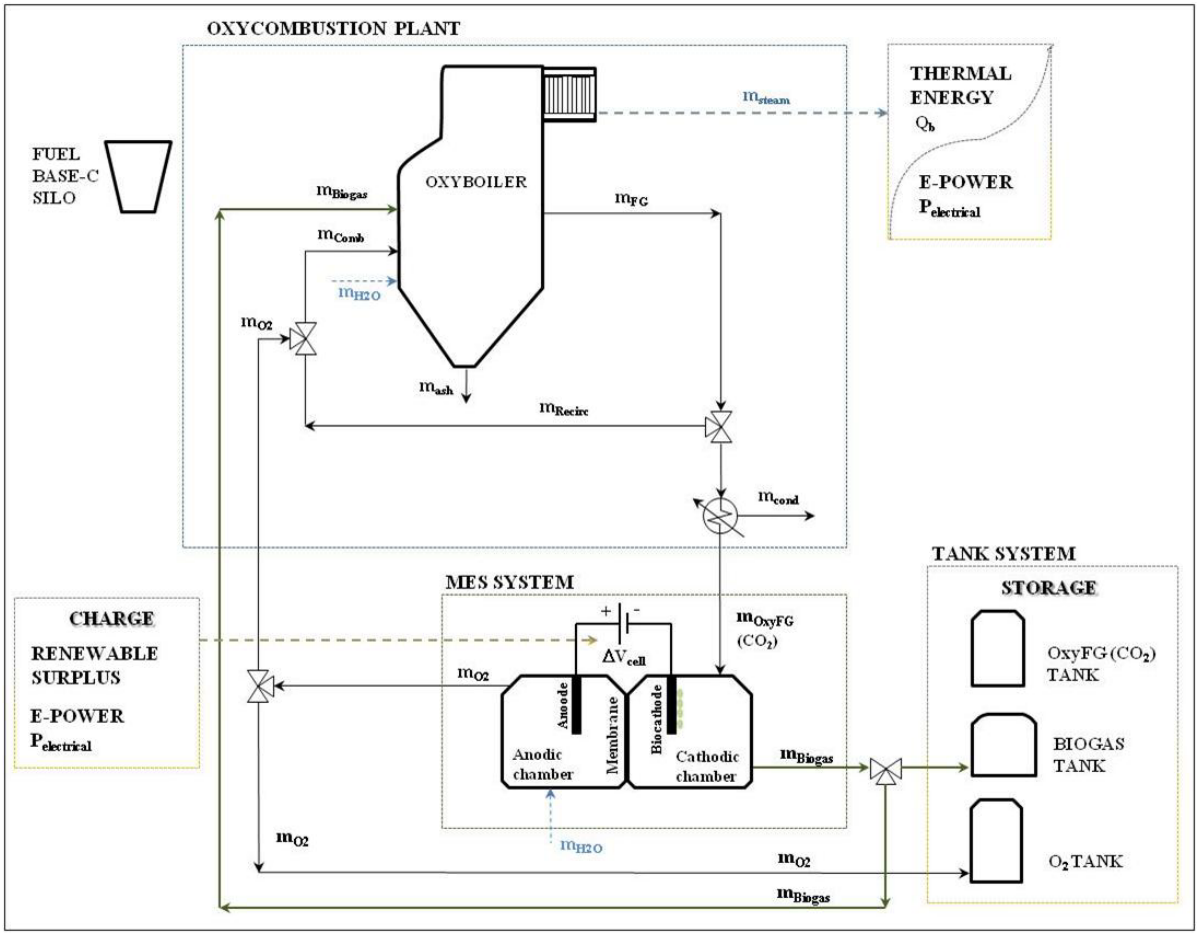

Fig 9. 100% self-sustaining "*OxyMES*" scheme, fed with the biogas produced in the *MES* cell (option C Table 6).

After this preliminary comparative analysis, it is concluded that **an *OxyMES* system provides the energy storage function without energetically penalizing the process** if it

546 is compared with an oxycombustion plant with conventional CO_2 capture. From the energy
547 point of view, the best option for the implementation of the *OxyMES* scheme would be to
548 apply it as a measure to decarbonize an industry, switching the original fuel of the
549 oxycombustion boiler to the biogas generated in the *MES* cell (future study), Fig. 9. This
550 also allows this industry to store RES surplus and consider new business models that
551 generate benefits derived from the energy storage market, which is currently undergoing
552 not only technical but also regulatory development [49]. With this option, the industry
553 would be closer to a circular economy and converted into a *net-negative-emissions*
554 *technology* system (*NET* system).
555 The second most favourable option for the *OxyMES* implementation would be to use it as a
556 system for neutralizing the CO_2 emissions of an industry by means of its conversion to
557 biomethane and then, to inject it to the gas network.
558 The *OxyMES* system has intrinsic advantages in that it produces biogas and oxygen in a
559 single-step system ('*all-in-one*'), while other *power-to-gas* systems require two
560 intermediate steps each with their corresponding equipment (electrolyzer and methanizer)
561 [50]. Regardless, the production of oxygen in microbial systems represents one of the
562 greatest challenges facing *MES* technologies due to the high CAPEX required to achieve
563 stable membranes and anodes [51]. It is expected that the *OxyMES* capabilities are
564 maximized when it is integrated into larger systems forming hubs of different industrial
565 processes [41].
566

567 **4. CONCLUSIONS**

568 In this study, a novel scheme has been proposed for the storage of renewable electrical
569 energy surplus and for its conversion to biogas through the hybridization of a microbial

electrosynthesis system with an industrial process operating in oxycombustion. The biogas can be stored and later purified to be discharged to the natural gas network.

This research has calculated that the round-trip efficiency of certain *power-to-gas* systems based on *MES* cells when coupled to industrial processes are at the same order of magnitude as the most promising equivalent routes. This clarifies their potentiality and allows them to remain as part of the feasible energy storage portfolio and paves the way for their technological development. It is worth highlighting the great advantage of the *OxyMES* system based on microbial electrosynthesis. It is an *all-in-one* system, which means that it converts CO_2 to biogas and produces oxygen for oxy-fuel combustion all within a single system.

The proposed process has two main limitations, the necessary overpotentials in the cell that penalize the overall efficiency and the need for storage tanks for the process gases. With regard to overpotentials, it has been found that certain cell potentials that are already close to reality achieve acceptable performance. Regarding the tanks, with the proper sizing of the O_2, biogas, and CO_2 process tank system, it is possible to achieve 100% autonomy, free from external feedstock supplies.

Future studies could address the coupling of bottom cycles to the *OxyMES* process to produce dispatchable electricity in a *power-to-power* scheme. This would enable the industrial operator to participate in new electricity market models.

CRediT authorship contribution statement

Ruth Diego: Formal analysis, investigation, methodology, writing (original draft preparation, review & editing), visualization. **Antonio Morán**: Conceptualization, methodology, supervision, funding acquisition and writing (review & editing). **Luis M. Romeo**: Conceptualization, methodology, supervision and writing (review & editing).

Declaration of competing interest

The authors declare that they have no known competing financial interests or personal relationships that could have appeared to influence the work reported in this paper.

Fundings: This research was funded by the 'Ministerio de Ciencia e Innovación', project ref: PID2020-115948RB-I00, co-financed by FEDER funds.

Part of the research that gave rise to these results received funding from the Seventh Framework Program of the European Community (FP7/2007-2013) under grant agreement No. 268191.

Appendix A. Supplementary material

PDF file.

NOMENCLATURE

Abbreviations

ASU: Air Separation Unit

CAPEX: Capital Expenditures

CCGT: Combined Cycle Gas Turbine

CCS: CO_2 Capture and Storage

CO_2-to-CH_4 ratio = FC

CPU: Compression and Purification Unit

Current-to-methane efficiency = Faradaic efficiency = FE

kWh: Kilowatt hour

MEC: Microbial Electrolysis Cell

MES: Microbial Electrosynthesis System

MWh: Megawatt hour

MSW: Municipal Solid Waste

NG: Natural Gas

OxyFG: Oxycombustion Flue Gases

OPEX: Operational Expenditures

PEM: Proton Exchange Membrane

PtG: Power to Gas

PV: Photovoltaic

RES: Renewable Energy Sources

Symbols

F: Faraday constant, 96485 C/mol e^-

HHV: Higher Heating Value [kJ/kg]

LHV: Lower Heating Value [kJ/kg]

M: molecular weight [g/mol]

m: mass flow [kg/h] or [t/h]

η: efficiency (%)

NHE: Normal Hydrogen Electrode (V)

Q: thermal power [MW_{th}]

SHE: Standard Hydrogen Electrode (V)

ΔV: external applied voltage [V]

W: specific energy consumption [kWh_e/kWh_{th}]

Subscripts:

b: boiler

e: electricity

f: oxycombustion plant fuel (coal)

d.b.: dry basis

w.b.: wet basis

vol: by volume

th: thermal

wth: weight

REFERENCES

[1] IEA (2020), World Energy Outlook 2020, IEA, Paris, [accessed 25.06.22].

[2] Regulation (EU) 2021/1119 of the European Parliament and of the Council of 30 June 2021 establishing the framework for achieving climate neutrality and amending Regulations (EC) No 401/2009 and (EU) 2018/1999 ('European Climate Law'). PE/27/2021/REV/1, [accessed 25.06.22].

[3] Directive (EU) 2018/2001 of the European Parliament and of the Council of 11 December 2018 on the promotion of the use of energy from renewable sources (Text with EEA relevance) PE/48/2018/REV/1, [accessed 25.06.22].

[4] California ISO (CAISO) Fast Facts: Impacts of renewable energy on grid operations. 2017. Retrieve from: http://www.caiso.com/informed/Pages/ManagingOversupply.aspx, [accessed 25.06.22].

[5] Blanco H, Faaij A, A review of the role of storage in energy systems with a focus on power to gas and long-term storage. Renewable and Sustainable Energy Reviews 2018; 81 (1): 1049-1086. https://doi.org/10.1016/j.rser.2017.07.062.

[6] ETIP-SNET. Position Paper. Smart Sector Integration, towards an EU System of

Systems Building blocks, enablers, architectures, regulatory barriers, economic assessment. July 2021. Retrieved from: https://www.etip-snet.eu/new-etip-snet-position-paper-smart-sector-integration-towards-eu-system-systems/, [accessed 25.06.22].

[7] EASE Report. Energy Storage Applications Summary. June 2020. Retrieved from: https://ease-storage.eu/publication/energy-storage-applications-summary/. [accessed 25.06.22].

[8] Ritchie H, Roser M. CO_2 and Greenhouse Gas Emissions. Published online at OurWorldInData.org. 2020. Retrieved from: 'https://ourworldindata.org/co2-and-other-greenhouse-gas-emissions' [Online Resource], [accessed 25.06.22].

[9] Olah G A, Goeppert A, Surya Prakash G K. Beyond Oil and Gas: The Methanol Economy. Wiley-VCH, 3rd ed. 2018. Weinheim, Germany. ISBN: 978-3-527-80567-9.

[10] Cotton C AR, Claassens N J, Benito-Vaquerizo S, Bar-Even A. Renewable methanol and formate as microbial feedstocks. Current Opinion in Biotechnology 2020; 62:168-180. https://doi.org/10.1016/j.copbio.2019.10.002.

[11] Bajracharya S, Sharma M, Mohanakrishna G, Dominguez Benneton X, Strik D PBTB, Sarma P M, Pant D, An overview on emerging bioelectrochemical systems (BESs): Technology for sustainable electricity, waste remediation, resource recovery, chemical production and beyond. Renewable Energy 2016; 98:153-170. https://doi.org/10.1016/j.renene.2016.03.002.

[12] Bajracharya S, Srikanth S, Mohanakrishna G, Zacharia R, Strik D PBTB, Pant D. Biotransformation of carbon dioxide in bioelectrochemical systems: State of the art and future prospects. Journal of Power Sources 2017; 356:256-273. https://doi.org/10.1016/j.jpowsour.2017.04.024

[13] Salimijazi F, Kim J, Schmitz A.M, Grenville R., Bocarsly A, Barstow B. Constraints on the efficiency of engineered electromicrobial production. Joule 2020; 4 (10): 2101–

695 2130. https://doi.org/10.1016/j.joule.2020.08.010.
696 [14] Villano M, Aulenta F, Ciucci C, Ferri T, Giuliano A, Majone M. Bioelectrochemical
697 reduction of CO_2 to CH_4 via direct and indirect extracellular electron transfer by a
698 hydrogenophilic methanogenic culture. Bioresource Technology 2010; 101 (9): 3085-3090.
699 https://doi.org/10.1016/j.biortech.2009.12.077
700 [15] Cheng S, Xing D, Call DF, Logan BE. Direct biological conversion of electrical
701 current into methane by electromethanogenesis. Environmental Science & Technology
702 2009; 43 (10): 3953-3958, https://doi.org/10.1021/es803531g
703 [16] Azizan N A Z, Kamyab H, Yuzir A, Abdullah N, Vasseghian Y, Ali I H, Elboughdiri
704 N, Sohrabia M. The selectivity of electron acceptors for the removal of caffeine, gliclazide,
705 and prazosin in an up-flow anaerobic sludge blanket (UASB) reactor. Chemosphere 2022;
706 303 (1): 134828. https://doi.org/10.1016/j.chemosphere.2022.134828.
707 [17] Gomez Vidales A, Omanovic S, Tartakovsky B. Combined energy storage and
708 methane bioelectrosynthesis from carbon dioxide in a microbial electrosynthesis system.
709 Bioresource Technology Reports 2019; 8:100302.
710 https://doi.org/10.1016/j.biteb.2019.100302
711 [18] Quan L M, Kamyab H, Yuzir A, Ashokkumar V, Hosseini S E, Balasubramanian B,
712 Kirpichnikova I. Review of the application of gasification and combustion technology and
713 waste-to-energy technologies in sewage sludge treatment. Fuel 2022; 316: 123199.
714 https://doi.org/10.1016/j.fuel.2022.123199.
715 [19] Lockwood, T. Developments in oxyfuel combustion of coal. IEA Clean Coal Centre
716 Report 2014. ISBN: 978–92–9029–561-7.
717 [20] Bailera M, Lisbona P, Romeo L M. Power to gas-oxyfuel boiler hybrid systems.
718 International Journal of Hydrogen Energy 2015; 40 (32): 10168-10175.
719 https://doi.org/10.1016/j.ijhydene.2015.06.074.

720 [21] Bailera M, Kezibri N, Romeo L M, Espatolero S, Lisbona P, Bouallou C. Future
721 applications of hydrogen production and CO_2 utilization for energy storage: Hybrid Power
722 to Gas-Oxycombustion power plants. International Journal of Hydrogen Energy 2017; 42
723 (19): 13625-13632. https://doi.org/10.1016/j.ijhydene.2017.02.123.
724 [22] Faria D G, Carvalho M MO, Neto M RV, de Paula E C, Cardoso M, Vakkilainen E K.
725 Integrating oxy-fuel combustion and power-to-gas in the cement industry: A process
726 modeling and simulation study. International Journal of Greenhouse Gas Control 2022;
727 114: 103602. https://doi.org/10.1016/j.ijggc.2022.103602.
728 [23] Rispoli A L, Verdone N, Vilardi G. Green fuel production by coupling plastic waste
729 oxy-combustion and PtG technologies: Economic, energy, exergy and CO_2-cycle analysis.
730 Fuel Processing Technology 2021; 221: 106922.
731 https://doi.org/10.1016/j.fuproc.2021.106922.
732 [24] Bailera M, Lisbona P, Romeo LM, Espatolero S. Power to Gas projects review: Lab,
733 pilot, and demo plants for storing renewable energy and CO_2. Renewable and Sustainable
734 Energy Reviews 2017; 69: 292-312. https://doi.org/10.1016/j.rser.2016.11.130.
735 [25] Aryal N, Kvist T, Amman F, Pant D, Ottosen L DM. An overview of microbial biogas
736 enrichment. Bioresource Technology 2018; 264: 359-369.
737 https://doi.org/10.1016/j.biortech.2018.06.013.
738 [26] Stanger R, Wall T, Spörl R, Paneru M, Grathwohl S, Weidmann M, Scheffknecht G,
739 McDonald D, Myöhänen K, Ritvanen J, Rahiala S, Hyppänen T, Mletzko J, Kather A,
740 Santos S. Oxyfuel combustion for CO_2 capture in power plants. International Journal of
741 Greenhouse Gas Control 2015; 40: 55-125. https://doi.org/10.1016/j.ijggc.2015.06.010.
742 [27] BOE-A-2018-14557 Resolución de 8 de octubre de 2018, de la Dirección General de
743 Política Energética y Minas, por la que se modifican las normas de gestión técnica del

744 sistema NGTS-06, NGTS-07 y los protocolos de detalle PD-01 y PD-02. Ministerio para la
745 Transición Ecológica 2018.
746 [28] Diego R, López C, Navarrete B, Coca T, López LA. CIUDEN PC Boiler
747 Technological Development in Power Generation. 2nd IEAGHG Oxyfuel Combustion
748 Conference 2011, Yeppoon, Australia.
749 [29] FP7-ENERGY European Commission Funding Project. Reliable and Efficient
750 Combustion of Oxygen/Coal/Recycled Flue Gas Mixtures (RELCOM Project), [accessed
751 25.06.22].
752 [30] Geppert F, Liu D, van Eerten-Jansen M, Weidner E, Buisman C, Ter Heijne A.
753 Bioelectrochemical Power-to-gas: State of the Art and Future Perspectives. Trends
754 Biotechnology 2016; 34 (11): 879-894. https://doi.org/10.1016/j.tibtech.2016.08.010.
755 [31] Mateos R, Escapa A, San-Martín MI, De Wever H, Sotres A, Pant D. Long-term open
756 circuit microbial electrosynthesis system promotes methanogenesis. Journal of Energy
757 Chemistry 2020; 41: 3-6. https://doi.org/10.1016/j.jechem.2019.04.020.
758 [32] Villano M, Ralo C, Zeppilli M, Aulenta F, Majone M. Influence of the set anode
759 potential on the performance and internal energy losses of a methane-producing microbial
760 electrolysis cell. Bioelectrochemistry 2016; 107: 1-6.
761 https://doi.org/10.1016/j.bioelechem.2015.07.008.
762 [33] Batlle-Vilanova P, Dissertation PhD: Bioelectrochemical transformation of carbon
763 dioxide to target compounds through microbial electrosynthesis. University of Girona
764 2016. https://dugi-doc.udg.edu/handle/10256/13415.
765 [34] Pelaz G, Carrillo-Peña D, Morán A, Escapa A. Electromethanogenesis at medium-low
766 temperatures: Impact on performance and sources of variability. Fuel 2022; 310 (A):
767 122336. https://doi.org/10.1016/j.fuel.2021.122336.

768 [35] Spiess S, Sasiain A, Waldmann N, Neuhauser E, Loibner A P, Kieberger N,
769 Haberbauer M. Bioelectrochemical Methanation of CO_2 from Untreated Steel Mill Gas.
770 Proceeding from 5th European Meeting of the International Society for Microbial
771 Electrochemistry and Technology (ISMET) 2021. Girona, Spain. https://euismet2021.eu/.
772 [36] California ISO (CAISO). The Renewables Watch Report: Wind and Solar Curtailment
773 December 29, 2021, [accessed 25.06.22].
774 [37] REE. Reunión Extraordinaria del Grupo de Seguimiento de la planificación. Estudios
775 de prospectiva del sistema y necesidades para su operabilidad. 29/09/2020, [accessed
776 25.06.22].
777 [38] Escudero A I, Espatolero S, Romeo L M, Lara Y, Paufique C, Lesort A-L, Liszka. M
778 Minimization of CO_2 capture energy penalty in second generation oxy-fuel power plants.
779 Applied Thermal Engineering 2016; 103: 274-281.
780 https://doi.org/10.1016/j.applthermaleng.2016.04.116.
781 [39] Zhou H, Xing D, Xu M, Su Y, Ma, J, Angelidaki I, Zhang Y. Optimization of a newly
782 developed electromethanogenesis for the highest record of methane production. Journal of
783 Hazardous Materials 2021; 407: 124363. https://doi.org/10.1016/j.jhazmat.2020.124363.
784 [40] Beese-Vasbender PF, Grote JP, Garrelfs J, Stratmann M, Mayrhofer KJ. Selective
785 microbial electrosynthesis of methane by a pure culture of a marine lithoautotrophic
786 archaeon. Bioelectrochemistry 2015; 102: 50–55.
787 https://doi.org/10.1016/j.bioelechem.2014.11.004.
788 [41] ETIP SNET Report. VISION 2050 Integrating Smart Networks for the Energy
789 Transition: Serving Society and Protecting the Environment. 2018. Retrieved from:
790 https://www.etip-snet.eu/etip-snet-vision-2050/, [accessed 25.06.22].
791 [42] Chen S, Patil S A, Brown R K, Schröder U. Strategies for optimizing the power output
792 of microbial fuel cells: Transitioning from fundamental studies to practical

793 implementation. Applied Energy 2019; 233–234: 15-28.
794 https://doi.org/10.1016/j.apenergy.2018.10.015.
795 [43] Thema M, Bauer F, Sterner M. Power-to-Gas: Electrolysis and methanation status
796 review. Renewable and Sustainable Energy Reviews 2019; 112: 775-787.
797 https://doi.org/10.1016/j.rser.2019.06.030.
798 [44] Frank E, Gorre J, Ruoss F, Friedl M J. Calculation and analysis of efficiencies and
799 annual performances of Power-to-Gas systems. Applied Energy 2018; 218: 217-231.
800 https://doi.org/10.1016/j.apenergy.2018.02.105.
801 [45] Nuortimo K, Eriksson T, Kuivalainen R, Härkönen J, Haapasalo H, Hyppänen T.
802 Tackling boundaries of CCS in market deployment of second-generation oxy-fuel
803 technology. Clean Energy 2018; 2 (1): 72–81. https://doi.org/10.1093/ce/zky002.
804 [46] Perrin N, Dubettier R, Lockwood F, Tranier J-P, Bourhy-Weber C, Terrien P.
805 Oxycombustion for coal power plants: Advantages, solutions and projects. Applied
806 Thermal Engineering 2015; 74: 75-82.
807 https://doi.org/10.1016/j.applthermaleng.2014.03.074.
808 [47] Bauer F, Hulteberg C, Persson T, Tamm D. Biogas upgrading - Review of commercial
809 technologies. Svenskt Gastekniskt Center AB. SGC Rapport 2013; Vol. 270. Retrieved
810 from: http://www.sgc.se/ckfinder/userfiles/files/SGC270.pdf
811 [48] Espatolero S, Romeo LM. Optimization of oxygen-based CFBC technology with CO_2
812 capture. Energy Procedia 2017; 114: 581-588.
813 [49] EASE. The Ancillary Services Report. 2021. Available on-line: https://ease-
814 storage.eu/publication/ancillary-services/, [accessed 25.06.22].
815 [50] Ipsakis D, Varvoutis G, Lampropoulos A, Papaefthimiou S, Marnellos G E,
816 Konsolakis M. Techno-economic assessment of industrially-captured CO_2 upgrade to
817 synthetic natural gas by means of renewable hydrogen. Renewable Energy 2021; 179:

818 1884-1896. https://doi.org/10.1016/j.renene.2021.07.109.

819 [51] Prévoteau A, Carvajal-Arroyo JM, Ganigué R, Rabaey K. (2020). Microbial

820 electrosynthesis from CO_2: forever a promise?. Current Opinion in Biotechnology 2020;

821 62: 48-57. https://doi.org/10.1016/j.copbio.2019.08.014.